J. metamorphic Geol., 2009, **27**, 41–54 doi:10.1111/j.1525-1314.2008.00802.x

Genesis of metapelitic migmatites in the Adirondack Mountains, New York

P. J. LANCASTER,[1]* B. FU,[1†] F. Z. PAGE,[1‡] N. T. KITA,[1] M. E. BICKFORD,[2] B. M. HILL,[2] J. M. McLELLAND[3] AND J. W. VALLEY[1]
[1]*Department of Geology and Geophysics, University of Wisconsin, 1215 W. Dayton St, Madison, Wisconsin 53706, USA (p.j.lancaster@bristol.ac.uk)*
[2]*Department of Earth Sciences, Syracuse University, 204 Heroy Geology Lab, Syracuse, New York 13244, USA*
[3]*Department of Geology, Colgate University, Hamilton, New York 12032, USA*

ABSTRACT Oxygen isotope ratios and rare earth element (REE) concentrations provide independent tests of competing models of injection *v.* anatexis for the origin of migmatites from amphibolite and granulite facies metasedimentary rocks of the Adirondack Mountains, New York. Values of $\delta^{18}O$ and REE profiles were measured by ion microprobe in garnet–zircon pairs from 10 sample localities. Prior U–Pb SIMS dating of zircon grains indicates that inherited cores (1.7–1.2 Ga) are surrounded by overgrowths crystallized during the Grenville orogenic cycle (~1.2–1.0 Ga). Cathodoluminescence imaging records three populations of zircon: (i) featureless rounded 'whole grains' (interpreted as metamorphic or anatectic), and rhythmically zoned (igneous) cores truncated by rims that are either (ii) discordant rhythmically zoned (igneous) or (iii) unzoned (metamorphic or anatectic). These textural interpretations are supported by geochronology and oxygen isotope analysis. In both the amphibolite facies NW Adirondacks and the granulite facies SE Adirondacks, $\delta^{18}O_{(Zrc)}$ values in overgrowths and whole zircon are highly variable for metamorphic zircon (6.1–13.4‰; $n = 95$, 10 μm spot). In contrast, garnet is typically unzoned and $\delta^{18}O_{(Grt)}$ values are constant at each locality, differing only between leucosomes and corresponding melanosomes. None of the analysed metamorphic zircon–garnet pairs attained oxygen isotope equilibrium, indicating that zircon rims and garnet are not coeval. Furthermore, REE profiles from zircon rims indicate zircon growth in all regions was prior to significant garnet growth. Thus, petrological estimates from garnet equilibria (e.g. *P–T*) cannot be associated uncritically with ages determined from zircon. The unusually high $\delta^{18}O$ values (> 10‰) in zircon overgrowths from leucocratic layers are distinctly different from associated metaigneous rocks ($\delta^{18}O_{(Zrc)} < 10‰$) indicating that these leucosomes are not injected magmas derived from known igneous rocks. Surrounding melanosomes have similarly high $\delta^{18}O_{(Zrc)}$ values, suggesting that leucosomes are related to surrounding melanosomes, and that these migmatites formed by anatexis of high $\delta^{18}O$ metasedimentary rocks.

Key words: Adirondacks; migmatite; oxygen isotopes; REE; zircon.

INTRODUCTION

Small, broadly granitic migmatite leucosomes are found commonly as layers or dyke-like structures, especially in high-grade metamorphic regions, and are the subject of an extensive literature (e.g. Ashworth & Brown, 1990; Brown *et al.*, 1995; Clemens & Droop, 1998; Brown, 2001; Ishihara, 2005). As 'migmatite' only implies a rock of mixed appearance (generally alternating light and dark layers), their genesis is frequently obscure. In metamorphic settings, both small-scale injection of externally derived melts and *in situ* anatexis can result in similar field appearances. One common approach to decipher these frequently complicated histories is to assume minerals such as garnet and zircon crystallized at the same time, so that thermobarometric information obtained from garnet equilibria may be 'dated' with U–Pb zircon crystallization ages.

Another method is to identify chemical signatures, such as oxygen isotope values ($\delta^{18}O$), which can discriminate between anatexis and injection, and suitable minerals to preserve them. Zircon is one such suitable mineral. A number of studies (e.g. Williams, 2001; Hanchar & Hoskin, 2003; Cavosie *et al.*, 2005, 2006; Valley *et al.*, 2005; Page *et al.*, 2007a,b; Ushikubo

**Present address*: Department of Earth Sciences, Bristol University, Wills Memorial Building, Queen's Road, Bristol BS8 1RJ, UK.
†*Present address*: School of Earth Sciences, University of Melbourne, Parkville, Victoria 3010, Australia.
‡*Present address*: Department of Geology, Oberlin College, 52 West Lorain Street, Oberlin, Ohio 44074, USA.

et al., 2008) have demonstrated the ability of zircon to incorporate useful tracer elements (e.g. U–Pb, O, Hf, Li, Ti and REE) and resist post-growth alteration.

In the case of oxygen, minerals crystallizing in a closed system will preserve their isotopic values despite partial melting or fractionation processes (Valley, 2003). Zircon growing in unaltered injected melts should therefore retain more mantle-like values [mantle $\delta^{18}O_{(Zrc)} = 5.3 \pm 0.6‰$, VSMOW; Valley *et al.*, 2005]. Migmatites frequently form in high-grade metapelites with high $\delta^{18}O$ shales as protoliths, so $\delta^{18}O_{(Zrc)}$ values over 10‰ are predicted, providing a clear distinction between the two sources. Zircon crystallizing in metasedimentary rocks surrounding injected melts will record variations in isotopic compositions because of the incorporation of the externally derived material, shifting $\delta^{18}O_{(Zrc)}$ values towards metapelitic compositions, typically higher than 6‰.

Zircon compositions are most informative in conjunction with data from other minerals with which zircon might have equilibrated and exchanged isotopically, such as garnet. For instance, oxygen isotope equilibrium between coeval garnet and zircon provides important constraints on reaction conditions during mineral growth. As garnet is resistant to oxygen isotopic resetting at temperatures up to 800 °C (Wright *et al.*, 1995; Valley, 2001; Clechenko & Valley, 2003; Vielzeuf *et al.*, 2005b), it frequently preserves growth zoning with little or no exchange by diffusion (see discussion in Peck & Valley, 2004; Vielzeuf *et al.*, 2005b). Traditional bulk analyses destroy information that might be obtained from this zoning, so *in situ* methods are preferable whenever possible. In addition, rare earth element (REE) profiles can be used to evaluate the relative timing of zircon and garnet growth, to test whether information from both minerals may be associated with the same event. REE diffusion in garnet is also very slow (Ganguly *et al.*, 1998; Tirone *et al.*, 2005), so grains will preserve their REE content from the time of crystallization. Zircon and garnet both have a strong preference for the heavy REE (HREE), but garnet is modally more abundant. Zircon growing coevally with or post-garnet crystallization will therefore preserve a distinctive decline in the HREE.

Oxygen analyses of bulk separates further characterize samples and allow direct comparison with the earlier work. Measurements of garnet and quartz can constrain peak temperatures and the scale of equilibration in metamorphic terranes. Care must be taken in feldspar-rich rocks, though, as quartz–feldspar oxygen exchange during cooling can be substantial (e.g. Valley, 2001; Peck & Valley, 2004). Analyses of whole rock powders ensure samples are representative of known units in the area.

In this study, we have applied ion microprobe analysis to zircon and garnet from migmatites in the Adirondack Mountains, New York. Here, layers of leucocratic material generally lie conformably within melanocratic metasedimentary units. As with most migmatites, the genesis of this relationship is ambiguous. Many leucocratic layers appear to be intrusive (i.e. formed by injection of unrelated magmas) because of sharp contacts between layers, but equally their origin could be *in situ* melting of adjacent metasedimentary rocks. Oxygen isotope values provide additional evidence for determining the genesis of these rocks. Values of whole rock $\delta^{18}O$ in metaigneous units across the region are rarely higher than 11‰ (VSMOW), whereas metasedimentary rocks are generally above 11‰ (Eiler & Valley, 1994; Valley *et al.*, 1994, 2005). Zircon and garnet crystallizing in granitoid leucosomes should therefore record considerably different values of $\delta^{18}O$ depending on whether the units were externally derived magmas or formed from anatexis of surrounding higher $\delta^{18}O$ metasedimentary rocks.

GEOLOGICAL BACKGROUND

Regional geology

The Adirondack Mountains represent a large exposure of the Grenville province in northern New York (Fig. 1). The region is divided into the upper amphibolite facies Lowlands in the NW and the granulite facies Highlands to the South and East, separated by the Carthage–Colton mylonite zone (CCZ). Previous workers have identified at least four major events as part of the Grenville orogenic cycle (e.g. Moore & Thompson, 1980; McLelland *et al.*, 1996, 2001, 2004; Wasteneys *et al.*, 1999; Selleck *et al.*, 2005; Heumann *et al.*, 2006). First, the Elzevirian orogeny at *c.* 1300 Ma incorporated a series of arc collisions and emplacement of juvenile calc-alkaline crust. It was followed by the Shawinigan orogeny at *c.* 1180 Ma, interpreted as a compressional event, followed by delamination of the lithosphere, resulting in a collapse of the over-thickened crust and the *c.*1155 Ma anorthosite–mangerite–charnockite–granite (AMCG) intrusive event, evidence of which is most prominent in the northeastern Adirondacks. The last key episode was the Ottawan orogeny at *c.* 1050 Ma, also a compressional event followed by delamination. Large extensional faults—including the CCZ—formed in response to this delamination, allowing the Lowlands to slide off the Highlands to the NW.

Previous work in the region includes studies of the petrology (Buddington, 1939; Wiener *et al.*, 1984), structural geology (McLelland & Isachsen, 1986), temperatures and pressures (e.g. Bohlen *et al.*, 1985; Kitchen & Valley, 1995; Spear & Markussen, 1997; Peck & Valley, 2004; Storm & Spear, 2005), geochronology (e.g. McLelland *et al.*, 1996, 2001, 2004; Heumann *et al.*, 2006; Bickford *et al.*, 2008), role of fluids (e.g. Valley *et al.*, 1990; Clechenko & Valley, 2003) and nature of anatexis (e.g. McLelland & Husain, 1986; Heumann *et al.*, 2006). In addition, oxygen isotope analysis of igneous bodies throughout the Grenville Province of southern Quebec, Ontario and

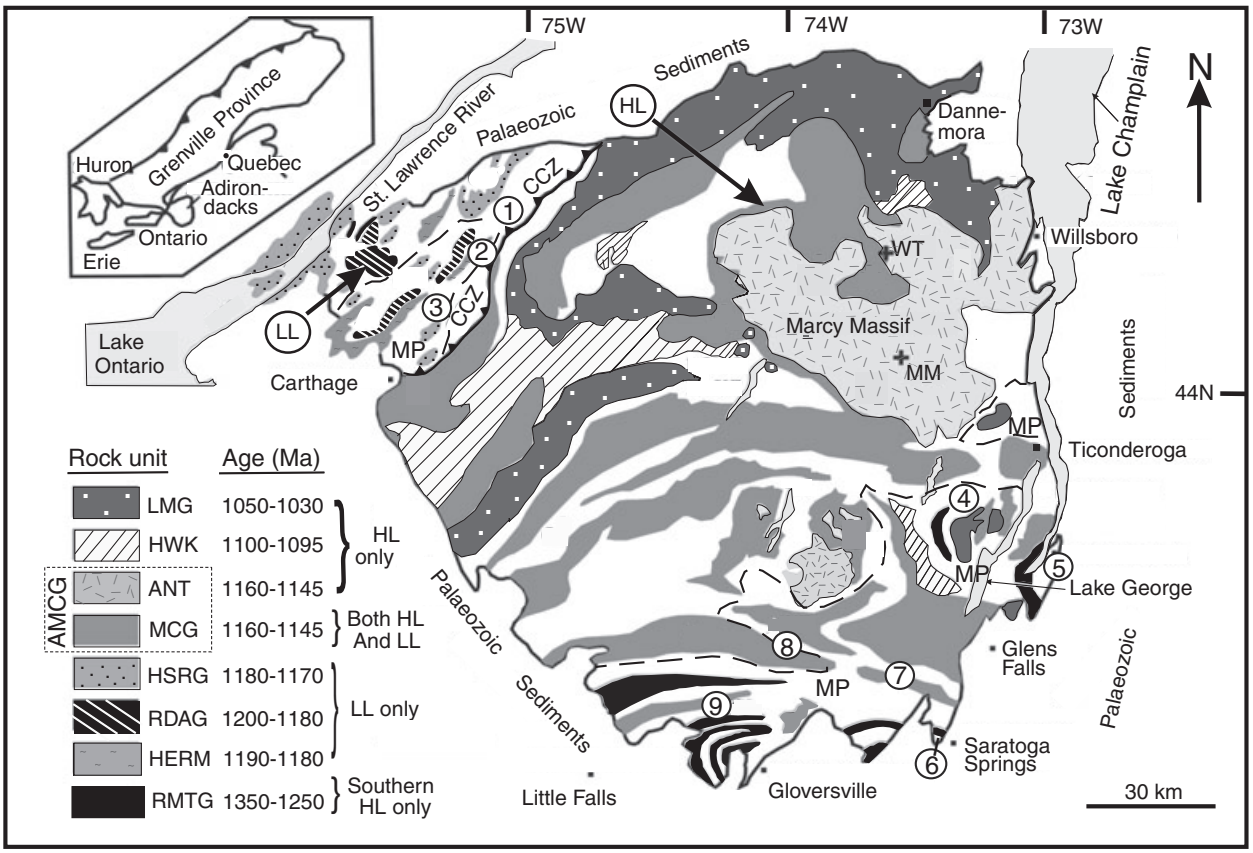

Fig. 1. Generalized geological map of the Adirondack Highlands (HL) and Lowlands (LL). Dashed lines define areas containing abundant migmatitic metapelite (MP). Abbreviations: CCZ, Carthage-Colton zone; ANT, anorthosite; MCG, mangerite-charnockite-granite suite; HSRG, Hyde School gneiss, Rockport granite; RDAG, Rossie diorite, Antwerp granitoid; H, Hermon granite; RMTG, Royal Mountain tonalitic granitoid. Unpatterned areas are underlain by undivided orthogneiss and metasedimentary rocks. Sample localities: (1) Devil's Elbow; (2) Foolish Dog; (3) Rt. 812; (4) Treadway Mt. (4a – site 1; 4b – site 2); (5) Comstock; (6) Daniel's Rd; (7) Conklingville Dam; (8) Pumpkin Hollow; (9) Pleasant Lake. After Heumann *et al.* (2006).

New York indicates many AMCG igneous rocks were intruded as high $\delta^{18}O$ magmas. Igneous granitic rocks to the west of the CCZ have elevated zircon and whole rock $\delta^{18}O$ compositions, indicating high $\delta^{18}O$ magmas up to ~11‰, whereas orthogneisses to the east rarely correspond to magmas with a $\delta^{18}O$ of ~12‰ (Morrison & Valley, 1988; Eiler & Valley, 1994; Valley *et al.*, 1994; Peck *et al.*, 2004).

Sample localities

Nine sample localities were studied, three in the NW Lowlands and six in the SE Highlands (Fig. 1; Table 1); full details are in File 1 in Supporting Information. One large outcrop in the SE Highlands, Treadway Mt., was sampled twice ~80 m apart to include both thickly and thinly layered material. These sample localities are the same as those studied in Heumann *et al.* (2006) and Bickford *et al.* (2008) (samples prefixed by MH-02 or BMH-01 and BMH-04, respectively) to permit direct correlation with their U–Pb zircon ages. In addition, several samples from Bickford *et al.* (2008) were provided for oxygen isotope analysis of mineral separates. Samples collected specifically for this study are prefixed either 05-ADK- or 06-ADK-, according to the year collected.

Migmatitic rocks in the upper amphibolite facies NW Lowlands are typically finely layered, with leucocratic layers varying from less than a millimetre near the CCZ to cm-scale in thickness further away. These units are predominantly composed of quartz + plagioclase + K-feldspar with a moderate number of garnet grains up to 2 mm (rarely up to 2 cm) in diameter. Melanocratic units normally dominate the outcrop, and are predominantly composed of quartz + biotite ± plagioclase ± K-feldspar with abundant garnet up to 3 mm in diameter. Monazite and zircon are found in all layers.

In the granulite facies SE Highlands, the leucocratic units sampled range in size from cm- to dm-scale bands and rarely cut across enclosing melanocratic members. The typical leucosome mineral assemblage is K-feldspar + blocky quartz + plagioclase ± garnet (≤5 mm) ± sillimanite ± titanite ± monazite ±

Table 1. Details of sample locations and numbers.

Location	Figure 1	GPS (18T)	Sample numbers
Lowlands			
Devil's Elbow	1	0478051 4911868	05-ADK-32 06-ADK-11 to -15 MH-02-19
Foolish Dog	2	0484713 4921286	05-ADK-23 to -25 06-ADK-01 to -10 MH-02-15a and -16b
Rt. 812	3	0469198 4898143	05-ADK-26 06-ADK-16 to -20 MH-02-09, -10a and -10b
Highlands			
Treadway Mt. #1	4	0612100 4843526	05-ADK-16 to -17 06-ADK-21 to -29 BMH-01-14
Treadway Mt. #2	4	0612066 4843611	05-ADK-18 to -19 06-ADK-30 to -35 BMH-04-06a to -06b
Comstock	5	0626242 4813825	05-ADK-20 to -21 06-ADK-36 to -40 BMH-04-02a to -02b
Daniel's Rd.	6	0599340 4773619	BMH-01-01a to -01b
Conklingville Dam	7	0587301 4796886	06-ADK-50 to -54 BMH-01-16
Pumpkin Hollow	8	0559807 4799636	05-ADK-14 06-ADK-55 to -59 BMH-01-20a to -20b
Pleasant Lake	9	0529063 4780942	05-ADK-29 06-ADK-46 to -49 BMH-01-12 MH-02-12

zircon; muscovite is rare. The melanosomes are similar in mineralogy but differ in modal abundance, consisting of quartz + plagioclase + K-feldspar + biotite + garnet (≤1 cm) ± sillimanite ± rutile ± monazite ± zircon.

METHODS

Up to 13, ~1 kg samples were collected from each of the 10 localities. Small (6 mm diameter × ~10 mm) plugs of rock were drilled from quartz- and garnet-rich domains and crushed to < 0.5 mm for hand picking mineral separates. Representative aliquots of leucocratic material were also cut from the slabs and powdered in a shatterbox with an alumina lining, and analysed for major and trace elements by X-ray fluorescence (XRF) at SGS Lakefield Research Laboratories, Toronto, Ontario, Canada.

Traverses to measure major element profiles were made across representative garnet grains in thin section by wavelength dispersive spectrometry (WDS) using a CAMECA SX51 electron microprobe at the University of Wisconsin–Madison (UW–Madison) and Probe for Windows software (Donovan *et al.*, 2007). Analytical conditions were 15 kV and 20 nA current, with a 10 s counting time on peak and 5 s counting time on either side of the peak. Spot size was 4 μm, and 5–10 analyses were made per grain. Standards were Gore Mtn. $Alm_{67}Py_{41}$ garnet for Al and Si, Rota (Hungary) And_{99} garnet for Ca, USNM Kakanui pyrope for Mg, Harvard Fe_2O_3 for Fe, synthetic Mn-olivine (Mn_2SiO_4) for Mn and TiO_2 for Ti.

Zircon was examined and photographed in cathodoluminescence (CL; for growth zoning) and secondary electron (SE; for surface features) imaging with a Hitachi S-3400N scanning electron microscope at UW–Madison, using a Gatan PanaCL/F imaging system and a 15 kV accelerating voltage; typical zircon images are shown in Fig. 2. As the garnet in thin section is not euhedral, it was checked for major element zoning in back-scattered electron (BSE) imaging to locate any offset or unusual zoning before detailed spot analyses by electron microprobe. After ion microprobe analysis, the bottoms of all SIMS pits were examined by SE imaging for inclusions and cracks which might affect the measured oxygen isotope ratios, and classified as 'regular' or 'irregular' (Cavosie *et al.*, 2005).

Oxygen isotope analysis by laser fluorination

Small aliquots (2.8–3.3 mg) of powdered leucosome prepared for XRF were analysed for whole rock $\delta^{18}O$ by laser fluorination. Samples of WR powder were not pre-treated in BrF_5 to avoid pre-reaction, but instead were evacuated overnight in an airlock chamber and individually moved under vacuum to the fluorination chamber for analysis (Spicuzza *et al.*, 1998b). Five aliquots of UWG-2 (Gore Mtn garnet standard) averaged 5.78 ± 0.10‰ (1 SD; 1 day of analyses), yielding a negligible correction of 0.02‰ relative to the accepted value of 5.80‰ (Valley *et al.*, 1995).

Garnet and quartz mineral separates were hand-picked from the crushed rock plugs, selecting for clarity and lack of visible inclusions or attached contamination. After garnet was removed from the sample, the remaining material was treated with concentrated HF for 60 s at 21 °C to frost the feldspar grains, aiding the selection of clean quartz. Aliquots of garnet and quartz weighing 0.7–3.0 mg were treated overnight in the sample chamber with BrF_5, then individually heated with a CO_2 laser in the presence of BrF_5 (Valley *et al.*, 1995; Spicuzza *et al.*, 1998a). All analyses were standardized against 3–5 analyses of UWG-2 per day ($\delta^{18}O$ = 5.80‰ VSMOW; Valley *et al.*, 1995) and reported in standard per mil (‰) notation relative to VSMOW. Thirty-two analyses of UWG-2 averaged 5.57 ± 0.07‰ (1 SD; eight days of analyses over 13 months), yielding an average correction of 0.23‰.

Oxygen isotope analysis by ion microprobe

Two standard 25 mm diameter epoxy zircon mounts were provided from the U–Pb ion microprobe studies of Heumann *et al.* (2006) and Bickford *et al.* (2008). A piece of KIM-5 zircon standard [$\delta^{18}O$ = 5.09‰; Valley, 2003] was mounted within 2 mm of the centre of each mount. Zircon was repolished to remove ion microprobe pits and a 300Å gold coat applied. *In situ* oxygen isotope measurements, each located as close to the original SHRIMP pits as possible, were made on

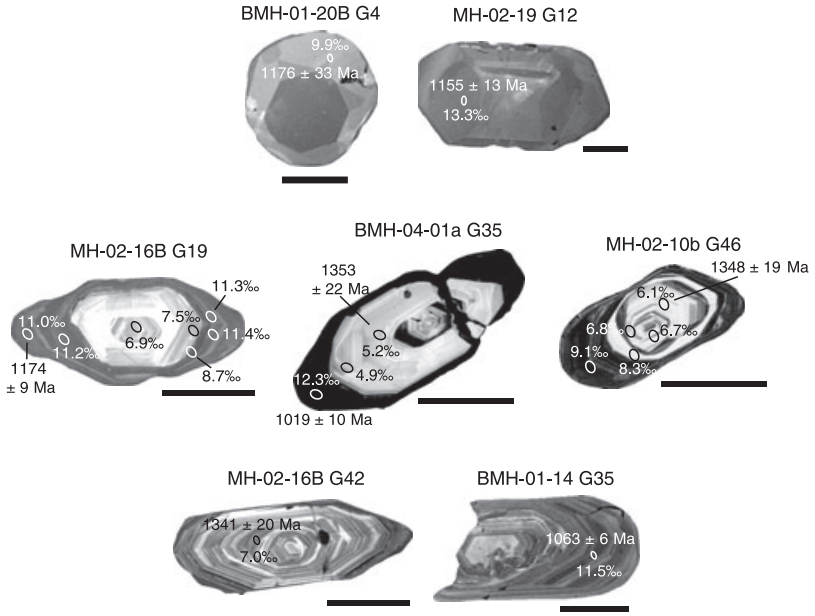

Fig. 2. Typical appearance in CL imaging for the three types of zircon prevalent in Adirondack migmatites, with previous U-Pb ages and new oxygen measurements indicated. Scale bars are 100 μm. Top row: rounded and sector-zoned whole metamorphic/anatectic zircon from Pumpkin Hollow leucosome (BMH-01-20B Grain 4) and Devil's Elbow (MH-02-19 Grain 12). Round habit, sector growth zoning or featureless with weak or no rhythmic banding. Middle row: Rhythmically zoned cores with minimally zoned rims from Foolish Dog melanosome (MH-02-16B Grain 19), Daniel's Rd. leucosome (BMH-04-01a Grain 35) and Rt. 812 melanosome (MH-02-10b Grain 46). Rhythmic oscillatory zoning in core characterized by regular, distinct variation between bright and dark bands in CL; igneous. Minimal zoning in overgrowth is metamorphic/anatectic. Bottom row: Multiple rhythmic zones, interpreted to be igneous, in zircon from Foolish Dog melanosome (MH-02-16B Grain 42) and Treadway Mt. 1 leucosome (BMH-01-14 Grain 35).

the Wisc–SIMS CAMECA IMS-1280 ion microprobe at UW–Madison using dual Faraday cup detectors. Each analysis required a total time of 4 min., including 10 s of pre-sputtering and ~60 s of automatic retuning of the secondary ions, and 80 s of analysis representing 20, 4-s measurement cycles. A Cs^+ primary ion beam, accelerated to 10 kV, was focussed to a diameter of ~10 μm on the sample surface. Secondary O^- ions were accelerated away from the sample by −10 kV and a normal-incidence electron gun was used for charge compensation. The secondary optics were configured in a manner similar to those in Kelly *et al.* (2007) and Page *et al.* (2007b) which aim to achieve high secondary ion transmission. The count rate for ^{16}O was $(1.7–2.8) \times 10^9$ cps depending on the primary beam intensity (~10^9 cps nA^{-1}), and the mass resolving power was set to ~2500.

Three sessions over two days in February 2006 resulted in 184 zircon analyses and 76 analyses of KIM-5 zircon standard. Blocks of 5–18 sample analyses were corrected by 6–8 measurements of KIM-5 bracketing each block. The average raw value of KIM-5 during the analytical period was 7.51 ± 0.15‰ (1 SD, n = 76; 1 SE = ±0.02%; IMF = 2.42‰), and the average spot-to-spot precision for groups of bracketing standard data is 0.17‰ (1 SD).

The majority of the oxygen isotope data in this study was obtained from zircon separated and dated by Heumann *et al.* (2006) and Bickford *et al.* (2008). These samples have the advantage that published geochronology provides age context to the oxygen isotope measurements. However, since a large volume of rock (~1 kg) was crushed to create the zircon separates for geochronology, textural information and coexisting mineral pairs were lost. To redress this problem, samples were collected from the same localities and zircon grains were identified in thin section which resembled those from the previous studies in shape and CL zoning.

Six thin sections used to measure garnet major element profiles were found to contain zircon within 5 mm of garnet. These thin sections were ground to 25 mm diameter, and UWG-2 and KIM-5 standards were face mounted and polished to enable *in situ* analysis by ion microprobe. Oxygen isotope analyses in garnet and zircon were measured at Wisc–SIMS in September and November 2006. Beam conditions and analytical corrections were the same as for the zircon grain mounts. The spot-to-spot precision of KIM-5 $\delta^{18}O$ analyses for the two sessions is ±0.23‰ (1 SD, n = 9) and ±0.34‰ (1 SD, n = 26). Each block of 6–11 garnet analyses was standardized against 8–10 bracketing analyses of UWG-2, with a spot-to-spot precision in bracketing UWG-2 data for the two sessions of 0.18‰ and 0.23‰ (1 SD), respectively. Each garnet analysis was then adjusted for differences in instrumental mass fractionation that result from solid solution.

The variable effect of mineral composition on instrumental mass fractionation (IMF) presents a major difficulty in accurate ion microprobe analysis of minerals with complex solid solutions such as garnet (e.g. Hervig *et al.*, 1992; Eiler *et al.*, 1997; Vielzeuf *et al.*, 2005a). Vielzeuf *et al.* (2005a) noted that in a large-radius, multi-collecting ion microprobe, the grossular content of garnet appears to exert the greatest effect on the IMF in garnet analyses, and speculated that the molar volume of garnet might be correlated with IMF. Vielzeuf *et al.* (2005a) developed a correction scheme that is based on a least-square calculation of IMFs from a set of standards that bracket the cation composition (specifically Ca, Fe^{2+} and Mg) of the unknown garnet. In this study, a set of six garnet standards (Table S1) was analysed during the same analysis session as the

Adirondack garnet. The standards span the range $Alm_{41–74}Pyp_{3–40}Grs_{1–31}Sps_{0–2}$, bracketing the sample garnet composition. The IMF of these standards was found to correlate with an estimate of their molar volume taken as the sum of published end-member molar volumes multiplied by their respective mole fractions, and a linear correction was established with a least-square best-fit line to these data (Fig. S1).

The cation composition of each sample garnet was measured by EMPA adjacent to each ion probe analysis (Tables S2 & S3), and the IMF was calculated for each analysis using the linear correction scheme. For these sample compositions, the IMF varies between −0.3‰ and −0.9‰ relative to the UWG-2 standard, and larger IMF corrections correlate with increasing Ca concentration. IMF calculated using the same standards and the method of Vielzeuf *et al.* (2005a) is systematically smaller by 0.1‰ on average with a maximum discrepancy of 0.3‰. The stated accuracy of the correction method of Vielzeuf *et al.* (2005a) is that it estimates the IMF of 75% of the standard suite to within ±0.6‰. The linear correction scheme used in this study reproduces the IMF from each of the six standards used to within ±0.4‰, on the same order as two standard deviations of the spot-to-spot uncertainty (0.4‰) by ion microprobe.

REE analysis by ion microprobe

Rare earth elements (La–Lu) and other selected trace elements (Ti, P, Y, Hf, Th & U) were measured by ion microprobe in zircon and garnet at Wisc–SIMS. A ~4nA O^- primary ion beam (23 kV total accelerating voltage) was shaped to a diameter of 20–25 μm on the sample surface. Analyses were conducted in monocollection mode using the axial ETP electron multiplier, applying a combination of energy filtering (40 eV) and high mass resolution (mass resolving power of 5000) as described in Page *et al.* (2007a).

Measured counts for each element were normalized to ^{30}Si, standardized to NIST 610 glass (Pearce *et al.*, 1997), and monitored with zircon standard 91500 (Wiedenbeck *et al.*, 2004). Because matrix differences between glass and zircon result in different relative ion yields, a correction factor of 1.25 was applied to the REE and Hf analyses in zircon when standardized to NIST 610 glass. No such correction was applied to garnet data. Considering the small correction to the absolute REE and Hf values in zircon, the absolute REE and Hf abundances in garnet may have an uncertainty of ~25%, which would not affect overall REE patterns.

RESULTS

Petrography and mineralogy

XRF analysis suggests broadly granitic and peraluminous compositions for all the leucocratic material examined in this study (Tables S4 & S5). In thin section, minerals in both leucosome and melanosome are foliated, with minerals such as mica and quartz wrapping around more resistant minerals such as garnet. CL imaging of zircon from both layers indicates two predominant morphologies: sector zoned rounded whole grains (top row, Fig. 2), interpreted as metamorphic or anatectic because of the lack of internal CL zoning and equant shape (Chiarenzelli & McLelland, 1993), and rhythmically zoned (igneous) cores truncated by unzoned (metamorphic or anatectic) rims (middle row). A third group of rhythmically zoned cores with discordantly zoned rims are a rare subset of this latter group, interpreted as igneous overgrowths on older igneous cores, based on their appearance in CL (bottom row).

Bulk analysis of oxygen isotopes

Values of $\delta^{18}O$ measured in powders of leucocratic whole rock are greater than 11‰ (11.6 to 15.0‰; Table 2), and are elevated relative to most granitic igneous rocks [$\delta^{18}O_{(WR)} < 11‰$]. For the leucosomes, all but two of the bulk garnet $\delta^{18}O$ values (42 of 44) are greater than 9‰, and most (37) are above 10‰. Similarly, in the melanosomes all but two of the 41 garnet samples have $\delta^{18}O_{(Grt)}$ values above 9‰, and 33 samples (80%) are >10‰. Bulk quartz measurements by laser fluorination are relatively homogeneous within each site locality (typical 1 SD = 0.24) and between corresponding leucosome–melanosome pairs of analyses. Of 102 analyses (57 in leucosomes and 45 in melanosomes), all but four samples (two each from leucosomes and melanosomes) have $\delta^{18}O_{(Grt)}$ values >12‰, and two-thirds are >13‰. Full results are presented in Fig. 3 and Table S6.

Apparent oxygen isotope temperatures were calculated from the laser fluorination data for quartz–garnet pairs, using the calibration for Alm–Pyp garnet (Valley *et al.*, 2003):

$$\Delta^{18}O_{(Qtz–Grt)} = \delta^{18}O_{(Qtz)} - \delta^{18}O_{(Grt)} = 2.71 \times (10^6/T^2).(T \text{ in K}) \quad (1)$$

If garnet and quartz equilibrated (i.e. no preserved growth zoning and no retrograde exchange), these $\Delta^{18}O_{(Qtz–Grt)}$ values should record peak temperatures during the final metamorphic event experienced by these samples. Apparent peak temperatures from leucosomes and melanosomes average 642 ± 63 °C (1 SD, n = 18) and 667 ± 57 °C (n = 14), respectively, in the NW Lowlands, and 667 ± 69 °C (n = 25) and 703 ± 163 °C (n = 26), respectively, in the SE Highlands (Table 2; Fig. 3). Analytical uncertainty in $\delta^{18}O$ by laser fluorination corresponds to ±40 °C for all samples. Thus, the apparent temperatures calculated from coexisting garnet and quartz are not statistically different between leucosome and

Table 2. Characterization of $\delta^{18}O$ in whole rock and minerals in migmatites across the Adirondack Mountains.

Location	Whole rock			Leucosome							Melanosome						
	SiO_2 (wt%)	$\delta^{18}O$ (‰)	$\Delta^{18}O_{(Grt\text{-}WR)}$ (‰)[a]	$\delta^{18}O$ Grt (‰)	1 SD	*n*	$\delta^{18}O$ Qtz (‰)	1 SD	*n*	*T* (°C)[b]	$\delta^{18}O$ Grt (‰)	1 SD	*n*	$\delta^{18}O$ Qtz (‰)	1 SD	*n*	*T* (°C)[b]
NW Lowlands																	
Devil's Elbow				12.1	0.5	6	15.2	0.2	6	662	12.1	0.8	4	15.2	0.1	4	662
Foolish Dog				10.3	0.2	8	13.8	0.2	11	602	10.4	0.2	6	13.7	0.2	9	641
Rt. 812				10.8	0.1	4	13.8	0.2	6	682	10.7	0.1	5	13.9	0.1	5	653
SE Highlands																	
Pleasant Lake	74.3[c]	14.8[c]	−2.1[c]	10.5	0.3	4	14.0	0.2	4	611	11.0	0.2	3	14.1	0.2	3	660
Pumpkin Hollow	74.0[c]	12.6[c]	−2.1[c]	9.4	0.1	3	12.8	0.5	4	613	9.1	0.1	3	12.4	0.3	3	643
Treadway #1	73.4	11.8	−2.1	9.9	0.7	5	12.8	0.2	10	687	9.5	0.9	5	12.9	0.2	6	622
Treadway #2	77.7	11.6	−2.4	9.0	1.5	3	12.6	1.2	4	601	10.4	0.9	6	13.2	0.8	6	716
Comstock	79.1	13.4	−2.4	11.1	0.1	6	14.1	0.3	6	687	11.2	0.2	4	14.0	0.1	4	704
Daniels Rd.				13.2		1	15.7		1	758	13.5		1	15.6		1	879
Conklingville Dam				10.5	0.4	4	13.7	0.2	5	651	10.7	0.3	4	13.7	0.2	4	679

Whole rock is XRF leucosome powder. Grt, garnet; Qtz, Quartz; n, number of samples. All oxygen ratios in permille (‰) relative to VSMOW. Full data sets presented in Table S6.
[a]Estimated equilibrium fractionation based on Eq. (2).
[b]Apparent temperature calculated from average $\Delta^{18}O_{(Qtz\text{–}Grt)}$ for each unit (Valley *et al.*, 2003); these are consistently lower than peak metamorphic temperatures.
[c]Average of two samples.

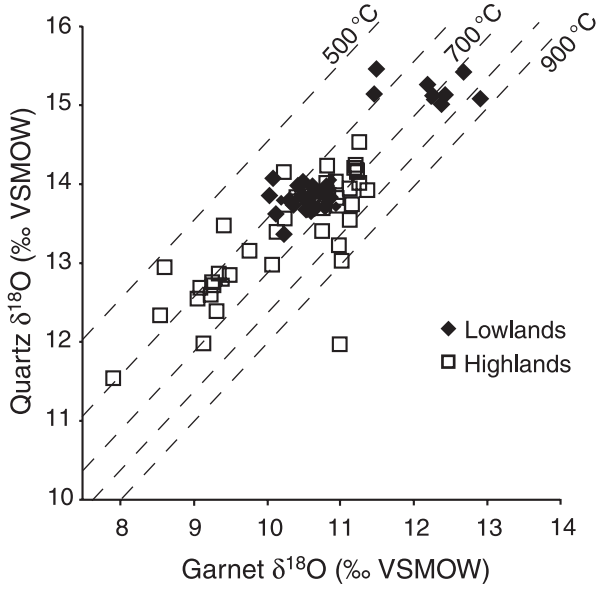

Fig. 3. Plot of $\delta^{18}O$ quartz *v.* $\delta^{18}O$ garnet measured by laser fluorination. Isotherms (Valley *et al.*, 2003) show that apparent temperatures are generally lower than the peak of metamorphism in the Adirondacks (700–750 °C), suggesting disequilibrium and retrograde exchange of quartz. A few samples record apparent temperatures higher than the peak of metamorphism, which are consistent with retrograde exchange in these feldspar-rich lithologies (Eiler *et al.*, 1993). Error bars are smaller than the symbol size.

melanosome, or between locations with differences of < 100 °C in peak metamorphic temperature, based on the standard deviations.

The apparent garnet–quartz temperatures are consistently lower than independent thermometry in the region (e.g. Bohlen *et al.*, 1985; Kitchen & Valley, 1995; Spear & Markussen, 1997; Peck & Valley, 2004; Storm & Spear, 2005), which records peak temperatures up to ~675 °C in the NW Lowlands and to ~800 °C in the SE Highlands. The low oxygen isotope temperatures might be attributed to retrograde exchange by diffusion; however, diffusion of oxygen in garnet is slow and closure temperatures are above 800 °C (Wright *et al.*, 1995; Valley, 2001; Clechenko & Valley, 2003; Vielzeuf *et al.*, 2005b). Thus, if retrograde exchange has occurred without recrystallization, as is suggested by textures and imaging, then diffusive exchange occurred between quartz and a third phase. The most likely other phase for exchange is feldspar, which would cause higher values of $\delta^{18}O_{(Qtz)}$ and erroneously low temperatures as seen in this study (Eiler *et al.*, 1993; Valley, 2001; Peck *et al.*, 2004). As thermometry was not the primary purpose of this study, microanalysis of quartz to investigate zoning or evidence for diffusion was not pursued.

In situ analysis of oxygen isotopes

The zoning observed in zircon by CL necessitated *in situ* ion microprobe techniques to obtain detailed information about individual growth stages, a decision supported by the highly variable oxygen results obtained in this study (Tables 3, 4 & S7; Fig. 4). Analyses of domains with concentric rhythmic growth zoning (mostly $\delta^{18}O_{(Zrc)}$ = 7–9‰) fall within the range of normal 'igneous' sources in the Adirondacks, whereas those in zircon with little to no CL zoning record a strong sedimentary signal (mostly 9–13‰). This difference supports the conclusion from CL imaging that the zircon cores are magmatic, surrounded by anatectic overgrowths.

In the NW Lowlands, igneous zircon cores in both leucosomes and melanosomes average $\delta^{18}O$ = 7.0 ± 1.4‰ (1 SD, *n* = 6) at Foolish Dog and 7.8 ± 1.1‰ (1 SD, *n* = 12) at Rt. 812; no igneous regions were identified by CL in zircon from Devil's Elbow. In contrast to the igneous cores, zircon

Table 3. Average $\delta^{18}O$ analyses of dated zircon compared to bulk garnet from each unit.

Location[a]	CL zoning[b]	Zrc $\delta^{18}O$ (‰)[c]	$\Delta_{(Zrc-Grt)}$ (‰)[d]	*t*-test[e]	
				95%	90%
Lowlands					
Devil's Elbow	meta	13.2 ± 0.2	1.1		
(MH-02-19)	ig	–			
Foolish Dog L	meta	10.2 ± 0.5	−0.1	n	n
(MH-02-15a)	ig	7.0 ± 1.8			
Foolish Dog M	meta	10.0 ± 0.8	−0.4		
(MH-02-16b)	ig	7.0 ± 0.1			
Rt. 812 L	meta	9.0 ± 1.4	−1.8	n	y
(MH-02-09)	ig	8.2			
Rt. 812 M	meta	7.8 ± 1.2	−2.9		
(MH-02-10)	ig	7.8 ± 1.1			
Highlands					
Pleasant Lake L	meta	11.2 ± 0.1	0.7	n	n
(BMH-01-12)	ig	11.5			
Pleasant Lake M	meta	11.5 ± 0.7	0.5		
(MH-02-06)	ig	7.7 ± 1.8			
Pumpkin Hollow L	meta	9.5 ± 0.4	0.1		
(BMH-01-20)	ig	10.5 ± 0.9			
Treadway Mt. #1 L	meta	11.6 ± 0.7	1.7	y*	y*
(BMH-01-14)	ig	10.2 ± 0.8			
Treadway Mt. #2 L	meta	7.3 ± 0.9	−1.7	y	y
(BM-04-06a)	ig	6.6 ± 0.7			
Treadway Mt. #2 M	meta	10.4 ± 0.8	−0.1		
(BM-04-06b1)	ig	9.9 ± 2.3			
Highlands					
Comstock L	meta	10.2 ± 1.0	−1.0	n	n
(BM-04-02a)	ig	7.8 ± 1.8			
Comstock M	meta	11.2 ± 0.1	0.0		
(BM-04-02b)	ig	9.3 ± 0.1			
Daniels Rd. L	meta	12.3 ± 0.4	−0.9	n	n
(BM-04-01a)	ig	7.2			
Daniels Rd. M	meta	12.5 ± 0.4	−1.0		
(BM-04-01b)	ig	6.8 ± 0.9			
Conklingville Dam L	meta	10.9 ± 1.2	0.4		
(BMH-01-16)	ig	7.2 ± 1.7			

Full details are available in Tables S6 (Grt), S7 (Zrc) and S12 (*t*-test).
[a]Location and sample number for dated zircon. L, leucosome; M, melanosome.
[b]Zoning pattern visible in cathodoluminescence (CL) imaging: meta, anatectic habit; ig, igneous habit.
[c]Zrc, zircon. Oxygen isotope ratios standardized to KIM–5 zircon standard, relative to VSMOW.
[d]Difference in oxygen isotope ratios between the anatectic zircon analyses and the average bulk garnet $\delta^{18}O$ (laser fluorination) from surrounding material.
[e]Summary of statistical *t*-test results comparing analyses in metamorphic zircon between leucosome and melanosome samples from each locality (y – statistically distinguishable, n – not distinguishable at given confidence level); see Tables S12.
*Compared to Treadway Mt. #2 M in the absence of dated zircon from Treadway Mt. #1 M.

overgrowths and whole grains recording anatectic growth in both leucosomes and melanosomes average $\delta^{18}O_{(Zrc)}$ = 13.2 ± 0.2‰ (1 SD, n = 5) at Devil's Elbow, 10.1 ± 0.6‰ (1 SD, n = 10) at Foolish Dog and 8.5 ± 1.4‰ (1 SD, n = 10) at Rt. 812. In the SE Highlands, much the same pattern was observed, with overgrowths up to 6‰ higher in $\delta^{18}O$ than corresponding cores (Table 3).

Almost universally, $\delta^{18}O$ values in zircon growth zones with anatectic zoning are higher than those with igneous zoning, and values in grains from melanocratic units are within error of those from leucocratic units. Grains zoned in CL display zoned variations in $\delta^{18}O_{(Zrc)}$, whereas unzoned grains are homogeneous over 2–3 analyses. There are only two exceptions to these observations. At the Rt. 812 locality, melanosome $\delta^{18}O_{(Zrc)}$ values are notably lower than in corresponding leucosomes (7.6‰ *v.* 8.2‰ in cores and 8.2‰ *v.* 9.3‰ in rims, respectively). At Treadway Mt., igneous and anatectic zircon in the leucosome have similar low values at sub-locality #2 (6.9‰ *v.* 7.1‰), but show the expected relation in similar lithologies, 80 m away at sub-locality #1 (10.0‰ in igneous zones *v.* 11.7‰ in anatectic zones). No differences were observed in zircon from leucocratic layers of different thicknesses within the same Treadway Mt. locality.

Table 4. Values of $\delta^{18}O$ for zircon measured in thin section by ion microprobe.

Location	Sample	L/M	CL zoning[a]	Zrc $\delta^{18}O$ (‰)[b]	1SD[c]
Highlands					
Treadway Mt. #2	06-ADK-35A Zrc #1.1	L	meta	8.2	0.2
	06-ADK-35A Zrc #1.2	L	ig	6.7	0.2
	06-ADK-35A Zrc #1.3	L	mixed	7.6	0.2
	06-ADK-35A Zrc #1.4	L	meta	8.0	0.2
	06-ADK-34D Zrc #1.1	M	ig	7.9	0.2
	06-ADK-34D Zrc #1.2	M	mixed	8.0	0.2
	06-ADK-34D Zrc #2.1	M	ig	9.1	0.2
	06-ADK-34D Zrc #2.2	M	meta	10.8	0.2
Conklingville Dam	06-ADK-50E Zrc #1.1	L	meta	7.7	0.1
	06-ADK-50E Zrc #1.2	L	ig	8.0	0.1

These analyses are paired with garnet $\delta^{18}O$ analyses in the same thin section by ion microprobe in Table 5.
L/M, leucosome/melanosome.
[a]Growth zone of analysis according to CL imaging. meta, anatectic habit; ig, igneous habit; mixed, pit included material from both zone types.
[b]Oxygen isotope ratios standardized to KIM-5 zircon standard relative to VSMOW.
[c]1 SD based on 8–10 bracketing standard analyses.

In contrast to the zircon analyses, most of the garnet grains measured in thin section were internally homogeneous. Three garnet crystals in two samples from Rt. 812 (NW Lowlands) have average $\delta^{18}O_{(Grt)}$ values of 10.8 ± 0.3‰ (2 SD; n = 40). Likewise, in the SE Highlands, eight garnet crystals from five localities have average $\delta^{18}O_{(Grt)}$ values of 7.8–13.2‰ (n = 5–21), whereas within-grain variability is typically ±0.3‰ (2 SD), on par with the uncertainty for individual analyses (±2 SD = 0.3–0.4‰). These oxygen values (Table S8) are broadly consistent with laser fluorination results that average a larger domain from the same locality. The primary exception is a ninth garnet from Treadway Mt. #2 melanosome (06-ADK-34D Grt #1), which records rim to core zoning in $\delta^{18}O_{(Grt)}$ of 8.0 to 10.2‰, respectively. It is improbable that only one garnet in this sample recorded retrograde alteration, so it is more likely that the large size of the grain (the second largest garnet studied *in situ*) prevented complete re-equilibration across growth boundaries at the peak of metamorphism and hence, some growth zoning was preserved.

REE profiles

To evaluate the timing of zircon growth relative to garnet, REE concentrations were measured in the same zircon growth zones as $\delta^{18}O$ (Tables S9 & S10; Fig. 5), paying particular attention to the relative

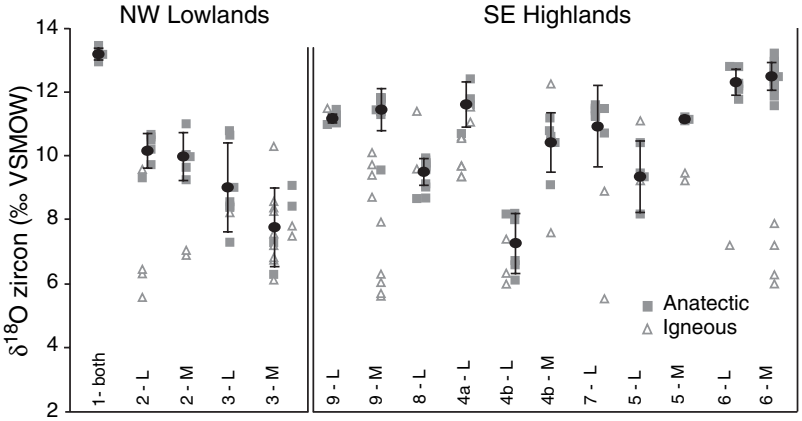

Fig. 4. Oxygen isotope ratios measured by ion microprobe in zircon. Anatectic average (filled ovals, ±1 SD) and measured data for anatectic (squares) and igneous (triangles) zircon classified by appearance of the analysed growth zone in CL imaging (see Fig. 2). Numbers at the bottom of the plot identify sample locality (Fig. 1). L, leucosome host; M, melanosome host. As the igneous measurements are primarily from inherited cores, the significant intra-sample scatter in values records differences between the original parent rocks. Scatter in the anatectic analyses is much smaller, and most likely records open system behaviour between growth events.

proportions of the HREE. Most zircon analyses record HREE-enriched profiles with positive Ce and negative Eu anomalies, although the magnitude of these deviations varies between samples. Twelve zircon crystals record elevated LREE concentrations [>1 relative to chondrites; Anders & Grevesse (1989)], especially in La, and flattened slopes in the LREEs, similar to the Type 2 (non-igneous) REE spectra of Cavosie *et al.* (2006), which struck inclusions of LREE-rich minerals (such as monazite or apatite). A smaller zircon subset, all from the Pumpkin Hollow locality, present HREE profiles with a negative slope, indicative of zircon growth during or after garnet growth (Rubatto & Hermann, 2007). Garnet REE patterns (Table S11; Fig. 5) are typically strongly depleted in LREE ($<10^{-1}$ relative to chondrites), rise steeply until Tb, and then either level off or decrease sharply in the HREE. Most garnet also records a moderate negative Eu anomaly, and a progressive depletion in HREE from core to rim.

DISCUSSION

Oxygen isotope ratios in garnet and zircon

Across the Adirondacks, garnet $\delta^{18}O$ values in these metasedimentary samples are >8‰ and mostly >10‰ (Fig. 6; Tables 2, 5, S6 & S8). Since the equilibrium fractionation in $\delta^{18}O$ between zircon and almandine-rich garnet ($\Delta^{18}O_{(Zrc–Grt)}$) is ~0.1‰ (Valley *et al.*, 2003)

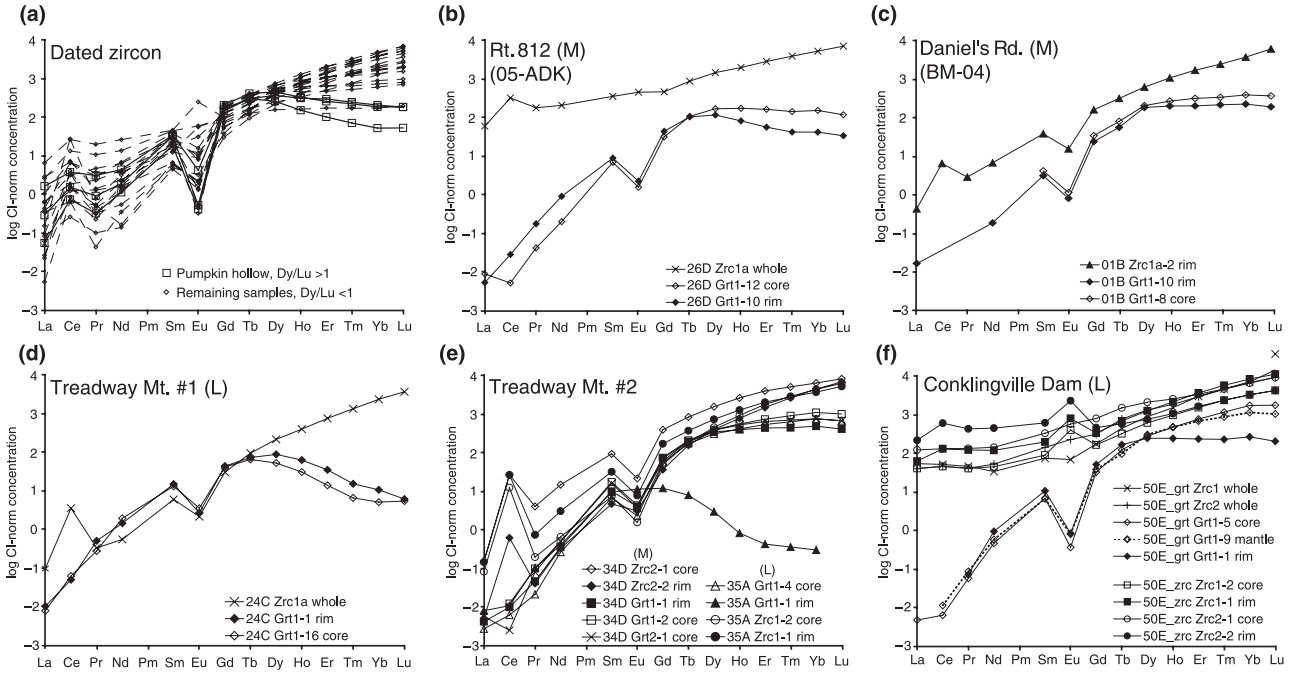

Fig. 5. Chondrite-normalized REE profiles (La–Lu) measured by ion microprobe in zircon and garnet. Each line represents a single analysis spot (Tables S9 & S10). (a) Previously dated zircon rim analyses. (b–f) Zircon and garnet analyses in thin section. All sample numbers prefixed with 06-ADK unless otherwise specified. L, leucosome; M, melanosome.

and the magmatic zircon–magmatic whole rock fractionation varies with wt% SiO_2 (Valley *et al.*, 2005), the fractionation between equilibrated garnet and granitic magma (whole rock, WR) can be estimated from the following equation:

$$\begin{aligned}\Delta^{18}O_{(Grt-WR)} &\cong \Delta^{18}O_{(Zrc-WR)} - 0.1\\ &= \delta^{18}O_{(Zrc)} - \delta^{18}O_{(WR)} - 0.1\\ &\cong -0.0612 \times (\text{wt\% } SiO_2) + 2.4 \quad (2)\end{aligned}$$

XRF analysis of leucocratic material from five samples in the SE Highlands yielded values of 73.4–79.1 wt% SiO_2, and equilibrium $\Delta^{18}O_{(Grt-WR)}$ values are estimated between −2.1‰ and −2.4‰ (Table 2). $\delta^{18}O_{(WR)}$ values in these same samples are 11.6 to 15.0‰, so $\delta^{18}O_{(Grt)}$ in equilibrium should be 9.2 to 12.9‰, overlapping values measured in garnet from corresponding rocks ($\delta^{18}O_{(Grt)}$ = 10.0 to 15.7‰). By contrast, typical values of $\delta^{18}O_{(WR)}$ measured in igneous intrusive rocks from the Adirondacks with similar silica contents (70.2 to 78.4 wt%) range from 9.9 to 11.4‰ (Eiler & Valley, 1994; Valley *et al.*, 1994), so equilibrated garnet should record $\delta^{18}O_{(Grt)}$ = 7.6 to 9.2‰. These igneous $\delta^{18}O_{(Grt)}$ values are considerably lower than those measured in garnet from this study, again suggesting disequilibrium with igneous material.

During anatexis, all new zircon grains or overgrowths crystallizing within small equilibrated domains should record the same value of $\delta^{18}O$ regardless of whether they crystallize in the melt or adjacent parent rocks. Statistical *t*-tests provide a measure of the degree of similarity between two $\delta^{18}O_{(Zrc)}$ data sets from corresponding leucosomes and melanosomes. Zircon compositions from Comstock, Foolish Dog, Pleasant Lake and Daniel's Rd. all fall below the critical *t*-test value at a 90% confidence limit, and thus their zircon populations cannot be distinguished based solely on their oxygen isotope ratios (Table 3, S12). Only at Treadway Mountain are anatectic overgrowths from leucosomes and melanosomes statistically different at the 2σ (95%) confidence level, suggesting they record two separate chemical environments during growth. Anatectic overgrowths on zircon from the leucosome at Treadway Mt. #2 averages $\delta^{18}O_{(Zrc)}$ = 7.3‰, whereas zircon from the melanosome averages $\delta^{18}O_{(Zrc)}$ = 10.4‰. Such low $\delta^{18}O_{(Zrc)}$ values in the leucosome resemble igneous units in the region, despite the featureless appearance of the analysed growth zones in CL, and indicate that this zircon did not crystallize in equilibrium with adjacent high $\delta^{18}O$ metasedimentary wall rocks. In contrast, the high $\delta^{18}O_{(Zrc)}$ average in the Treadway Mt. #1 leucosome ($\delta^{18}O_{(Zrc)}$ = 11.6‰) indicates a metasedimentary source.

A related matter is the relative timing of mineral growth. Zircon and associated 'peak' metamorphic minerals are frequently assumed to be coeval, such that U–Pb ages obtained from zircon can be combined with petrological information obtained from associated minerals. One might predict coeval growth of garnet and rims on zircon, as many melt-producing reactions also produce garnet (e.g. Spear *et al.*, 1999 and references therein). In fact, several studies in the Adirondacks have associated U–Pb zircon ages with garnet barometry to determine depth of burial at specific times (e.g. Mezger *et al.*, 1993; McLelland *et al.*, 2001; Alcock *et al.*, 2004). However, only four samples

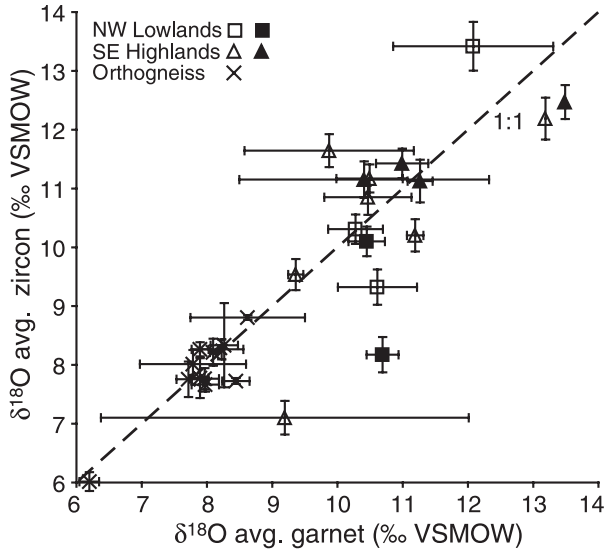

Fig. 6. Average zircon *v.* average garnet $\delta^{18}O$ measured in this study (□ and Δ), compared with orthogneiss zircons from Valley *et al.* (1994)(×). Uncertainties at 2 SD. All garnet analyses were by laser fluorination (Table 1), as were zircon analyses in Valley *et al.* (1994). Zircon from this study was analysed by ion microprobe, averaged across several spot analyses (Table 2). Open symbols represent leucosome samples; filled symbols are from melanosomes.

Table 5. Values of $\delta^{18}O$ of garnet measured in thin section by ion microprobe.

Location	Sample	L/M	Grs[a]	Alm[a]	Pyp[a]	Sps[a]	IMF[b]	Average $\delta^{18}O$ (‰)	1 SD
Lowlands									
Rt. 812	06-ADK-16A Grt #1	L	2.9	76.0	19.1	2.0	−0.8	10.4	0.3
	06-ADK-16A Grt #1	M	2.8	75.0	20.4	1.7	−0.8	10.7	0.2
	06-ADK-16A Grt #2	M	2.8	73.3	22.3	1.6	−0.8	10.5	0.1
Highlands									
Treadway Mt. #1	06-ADK-24C Grt #1	L	5.3	72.3	20.5	1.9	−0.6	9.9	0.3
Treadway Mt. #2	06-ADK-35A Grt #1	L	5.5	75.6	15.9	3.0	−0.5	7.7	0.6
	06-ADK-35A Grt #2	L	5.6	73.9	16.7	3.8	−0.5	7.6	0.3
	06-ADK-35A Grt #3	L	5.2	76.0	15.5	3.3	−0.5	7.5	0.4
	06-ADK-34D Grt #1	M	6.2	72.9	16.7	4.3	−0.4	8.4	0.7
	06-ADK-34D Grt #2	M	6.0	74.1	15.7	4.2	−0.5	8.0	0.2
Comstock	06-ADK-39A Grt #1	L	3.7	75.1	19.0	2.2	−0.7	10.7	0.2
Daniel's Rd.	BM-04-01B Grt #1	M	3.5	76.2	18.8	1.6	−0.7	12.8	0.2
Conklingville Dam	06-ADK-50E Grt #1	L	3.3	76.4	16.8	3.4	−0.7	10.1	0.3

L/M, leucosome/melanosome.
[a]Grs, grossular; Alm, almandine; Pyp, pyrope; Sps, spessartine. Major element analyses are in Tables S2 & S3.
[b]Correction applied to standardized $\delta^{18}O$ values (VSMOW) due to major element instrumental mass fractionation (IMF) calculated as 0.6779 × (molar volume) − 78.845.

in this study—Foolish Dog and Pumpkin Hollow leucosomes, and Treadway Mt. #2 and Comstock melanosomes—have $|\Delta^{18}O_{(Zrc–Grt)}|$ within analytical uncertainty of the equilibrium value at metamorphic temperatures (< 0.3‰) between averaged zircon rim and bulk garnet (Table 3).

Values of $\Delta^{18}O_{(Zrc–Grt)}$ approximating the equilibrium fractionation are a necessary condition to establish coeval growth or actual equilibrium exchange, but are not independently sufficient. The $\delta^{18}O$ of a rock will remain unchanged unless it interacts with an external source (e.g. fluid or melt). Thus, trace minerals growing at different times can record 'equilibrium' $\delta^{18}O$ values through exchange with the same rock. Likewise, disequilibrium values of $\Delta^{18}O_{(Zrc–Grt)}$ cannot be used to identify which mineral crystallized first. Another chemical tracer is needed to determine timing, such as REE profiles measured in co-existing zircon and garnet pairs.

REE profiles and distribution coefficients

Both zircon and garnet preferentially accept the HREE into their crystal structures, but garnet is typically more abundant, controlling the REE budget in a rock. Profiles in zircon grains crystallized in the absence of garnet generally have chondrite-normalized values that increase through the LREE and MREE, with positive Ce and negative Eu anomalies, and then either rise more slowly or level off through the HREE (Hinton & Upton, 1991). If anatectic zircon zones have profiles of this general shape, it would suggest the zircon grew prior to any substantial garnet growth. In zircon that grew synchronously with or later than garnet, however, REE profiles should be observed that are characteristically flattened or declining across the HREE (e.g. Hinton & Upton, 1991; Bea & Montero, 1999; Schaltegger *et al.*, 1999; Rubatto, 2002).

Zircon from the Pumpkin Hollow locality stand in stark contrast to the majority in this study, with profiles that decrease through the HREE ($Dy_{CI}/Lu_{CI} > 1$) instead of rising (Fig. 5). Three zircon rims record strongly depleted HREE patterns ($Dy_{CI}/Lu_{CI} > 2$; samples BMH-01-20A and -20B), whereas all other rims have $Dy_{CI}/Lu_{CI} < 1$ (Fig. 7; Table S9). These three rims have the smallest observed oxygen isotope fractionations between zircon and garnet ($|\Delta^{18}O_{(Zrc–Grt)}| <$ 0.5‰; Fig. 7), but are still not consistent with equilibrium ($|\Delta^{18}O_{(Zrc–Grt)}| < \sim$0.3‰). The steep negative slopes of the HREE profiles suggest the zircon rims grew after initial garnet growth, recording the preferential take-up of HREE into the chemical structure of more abundant garnet. The Pumpkin Hollow zircon rims all have similar U–Pb ages (1136–1176 Ma), suggesting that the REE profiles represent a single event. In all other respects, Pumpkin Hollow strongly resembles the other SE Highland localities, which have larger $|\Delta^{18}O_{(Zrc–Grt)}|$ values (> 0.5‰) and shallow HREE

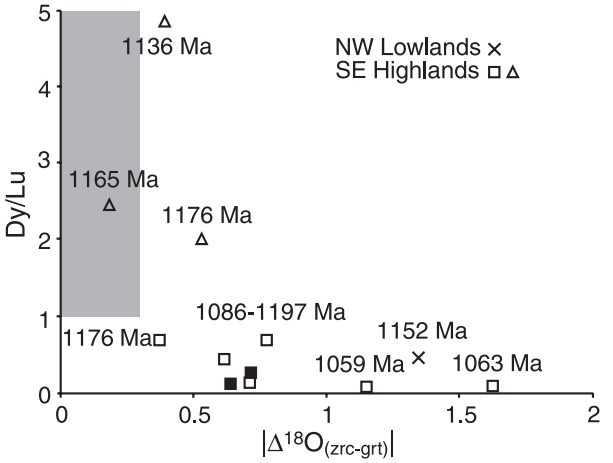

Fig. 7. Dy/Lu *v.* $|\Delta^{18}O_{(Zrc–Grt)}|$ in coexisting zircon and garnet pairs from thin sections. Highlands samples are divided into those from Pumpkin Hollow (Dy/Lu in zircon > 1; Δ) and all others (Dy/Lu < 1; □). Open symbols are from leucosome samples; closed symbols from melanosomes. Grey box indicates range suggesting equilibrium [$|\Delta^{18}O_{(Zrc–Grt)}| < 0.3‰$, Dy/Lu > 1].

zircon rim profiles, indicating zircon and garnet are not contemporaneous.

Grenville orogeny in the Adirondacks

Combining previous U–Pb ages with the new $\delta^{18}O$ and REE data resolves a long-standing question in the amphibolite facies NW Lowlands. Low values of water activity (a_{H2O}) are estimated for the peak of metamorphism (see Valley *et al.*, 1990), and yet estimates of metamorphic pressure and temperature are not sufficient for widespread dry melting unless unusual fluxes (such as boron) were important. If these estimates are correct, melting and the peak of metamorphism did not have to occur simultaneously. One solution to this enigma is if melting occurred during an earlier metamorphic event than is recorded by mineral thermometers. The analyses obtained in this study indicate that anatectic zircon rims grew prior to any significant garnet growth, confirming this suggestion. However, these results cannot rule out the possibility that the events represented by growth of anatectic zircon and later metamorphic garnet were part of a single, more complex orogeny that cannot be subdivided within the resolution of SIMS U–Pb geochronology.

These analyses also support the conclusion that the Adirondacks experienced at least four high temperature events in the Highlands and three in the NW Lowlands. The first formed the original igneous zircon, predominantly before or during the Elzevirian orogeny (*c.* 1300 Ma), now observed as relict cores. A second event, possibly the Shawinigan orogeny (*c.* 1180 Ma), led to the growth of anatectic rims on those zircon cores, as well as crystallizing new round whole grains. The intrusion of voluminous AMCG magmas

(anorthosite, mangerite, charnockite and granite) was a distinct third event that resulted in contact metamorphism throughout the Adirondacks at 1155 ± 5 Ma. The Shawinigan-age partial melting dehydrated the rocks, which were subsequently buffered at low a_{H2O} during the last regional scale metamorphism at *c*. 1050 Ma (Ottawan orogeny) in the Highlands.

CONCLUSIONS

The precision and small spot size of *in situ* ion microprobe analyses permit correlation of information from multiple elemental and isotope systems, testing whether coexisting minerals are cogenetic and leading to more complete rock histories. Wherever possible, the significance of coexisting minerals should be evaluated by independent geochemistry measured *in situ* from petrographic sections. In the Adirondack samples of this study, most conformable granitoid layers from both upper amphibolite and granulite facies migmatites represent anatectic melts of pelitic metasedimentary rocks that experienced at least four orogenic and magmatic episodes between 1300 and 1000 Ma. Oxygen isotope ratios in anatectic zircon overgrowths and garnet are much higher than values for most igneous rocks in the Adirondacks. These high $\delta^{18}O$ values are not consistent with formation of migmatites by injection of magma from known igneous sources. For all the samples in this study, oxygen isotope fractionations demonstrate that garnet and zircon did not equilibrate in Adirondack migmatites. However, these two parameters cannot determine the relative order of mineral crystallization. The positive slope of HREE analyses in zircon indicates that most zircon grew earlier than the garnet found within the same leucosome. Serious errors in interpretation could therefore result from correlating U–Pb zircon ages with 'peak' metamorphic pressures, temperatures or fluid conditions estimated from garnet equilibria.

ACKNOWLEDGEMENTS

The authors thank the following people for assistance: B. Hess, sample preparation; M. Spicuzza, laser fluorination; J. Fournelle, electron microprobe and SEM; T. Ushikubo and J. Kern, ion microprobe; and S. Wilson and N. Eck, field assistance. T. Vennemann, N. Kelley, J. Bowman and J. Craven provided constructive reviews and discussion. PJL was supported by a Weeks Research Assistantship, and in the field by Sigma Xi and GSA. NSF EAR0319230 and EAR0516725 support the Wisc–SIMS lab. JWV thanks NSF EAR0509639 and DOE 93ER14389.

REFERENCES

Alcock, J., Isachsen, C. E., Livi, K. & Muller, P., 2004. Unraveling growth history of zircon in anatectites from the northeast Adirondack Highlands, New York: Constraints on pressure-temperature-time-paths. In: *Proterozoic tectonic evolution of the Grenville orogen in North America (Memoir 197)* (eds Tollo, R.P., Corriveau, L., McLelland, J.M. & Bartholomew, M.J.), pp. 267–284. Geological Society of America, Boulder, CO.

Anders, E. & Grevesse, N., 1989. Abundances of the elements: meteoritic and solar. *Geochimica et Cosmochimica Acta*, **53,** 197–214.

Ashworth, J. & Brown, M., 1990. *High-Temperature Metamorphism and Crustal Anatexis*, 407 p. Mineralogical Society of Great Britain and Ireland, London.

Bea, F. & Montero, P., 1999. Behavior of accessory phases and redistribution of Zr, REE, Y, Th, and U during metamorphism and partial melting of metapelites in the lower crust: an example from the Kinzigite Formation of Ivrea-Verbano, NW Italy. *Geochimica et Cosmochimica Acta*, **63,** 1133–1153.

Bickford, M. E., McLelland, J. M., Selleck, B. W., Hill, B. M. & Heumann, M. J., 2008. Timing of anatexis in the eastern Adirondack Highlands: implications for tectonic evolution during ca. 1050 Ma Ottawan orogenesis. *Geological Society of America Bulletin*, **120,** 950–961.

Bohlen, S. R., Valley, J. W. & Essene, E. J., 1985. Metamorphism in the Adirondacks I: petrology, pressure, and temperature. *Journal of Petrology*, **26,** 971–992.

Brown, M., 2001. Orogeny, migmatites and leucogranites: a review. *Journal of Earth System Science*, **110,** 313–336.

Brown, M., Averkin, Y. A. & McLellan, E. L., 1995. Melt segregation in migmatites. *Journal of Geophysical Research*, **100,** 15655–15679.

Buddington, A. F., 1939. *Adirondack Igneous Rocks and Their Metamorphism (Memoir 7)*, 354 p. Geological Society of America, Boulder, CO.

Cavosie, A. J., Valley, J. W., Wilde, S. A. & EIMF, 2005. Magmatic $\delta^{18}O$ in 4400-3900 Ma detrital zircons: a record of the alteration and recycling of crust in the Early Archean. *Earth and Planetary Science Letters*, **235,** 663–681.

Cavosie, A. J., Valley, J. W., Wilde, S. A. & EIMF, 2006. Correlated microanalysis of zircon: Trace element, $\delta^{18}O$, and U-Th-Pb isotopic constraints on the igneous origin of complex >3900 Ma detrital grains. *Geochimica et Cosmochimica Acta*, **70,** 5601–5616.

Chiarenzelli, J. R. & McLelland, J. M., 1993. Granulite facies metamorphism, palaeo-isotherms, and disturbance of the U-Pb systematics of zircon in anorogenic plutonic rocks from the Adirondack Highlands. *Journal of Metamorphic Geology*, **11,** 59–70.

Clechenko, C. C. & Valley, J. W., 2003. Oscillatory zoning in garnet from the Willsboro Wollastonite Skarn, Adirondack Mts., New York: a record of shallow hydrothermal processes preserved in a granulite facies terrane. *Journal of Metamorphic Geology*, **21,** 771–784.

Clemens, J. D. & Droop, G. T. R., 1998. Fluids, *P–T* paths and the fates of anatectic melts in the Earth's crust. *Lithos*, **44,** 21–36.

Donovan, J. J., Kremser, D. & Fournelle, J. H., 2007. *Probe for Windows User's Guide and Reference, Enterprise Edition*, 355 p. Probe Software, Inc., Eugene, OR.

Eiler, J. M., Graham, C. M. & Valley, J. W., 1997. SIMS analysis of oxygen isotopes; matrix effects in complex minerals and glasses. *Chemical Geology*, **138,** 221–244.

Eiler, J. M. & Valley, J. W., 1994. Preservation of pre-metamorphic oxygen isotope ratios in granitic orthogneiss from the Adirondack Mts., N.Y. *Geochimica et Cosmochimica Acta*, **58,** 5525–5535.

Eiler, J. M., Valley, J. W. & Baumgartner, L. P., 1993. A new look at stable isotope thermometry. *Geochimica et Cosmochimica Acta*, **57,** 2571–2583.

Ganguly, J., Tirone, M. & Hervig, R. L., 1998. Diffusion kinetics of Samarium and Neodymium in Garnet, and a method for determining cooling rates of rocks. *Science*, **281,** 805–807.

Hanchar, J. M. & Hoskin, P. W. O. (eds.) 2003. Zircon. In: *Reviews in Mineralogy and Geochemistry*, Vol. 53. 500 p. Mineralogical Society of America, Washington, DC.

Hervig, R. L., Williams, P., Thomas, R. M., Schauer, S. N. & Steele, I. M., 1992. Microanalysis of oxygen isotopes in insulators by secondary ion mass spectrometry. *International Journal of Mass Spectrometry and Ion Processes*, **120,** 45–63.

Heumann, M. J., Bickford, M. E., Hill, B. M., McLelland, J. M., Selleck, B. W. & Jercinovic, M. J., 2006. Timing of anatexis in metapelites from the Adirondack lowlands and southern highlands: a manifestation of the Shawinigan orogeny and subsequent anorthosite-mangerite-charnockite-granite magmatism. *Geological Society of America Bulletin*, **118,** 1283–1298.

Hinton, R. W. & Upton, B. G. J., 1991. The chemistry of zircon: variations within and between large crystals from syenite and alkali basalt xenoliths. *Geochimica et Cosmochimica Acta*, **55,** 3287–3302.

Ishihara, S., 2005. *Fifth Hutton Symposium: The Origin of Granites and Related Rocks: Proceedings of a Symposium Held in Toyohashi, Japan*, 2–6 September 2003, 390 p. Geological Society of America, Boulder, CO.

Kelly, J. L., Fu, B., Kita, N. T. & Valley, J. W., 2007. Optically continuous silcrete quartz cements of the St. Peter Sandstone: high precision oxygen isotope analysis by ion microprobe. *Geochimica et Cosmochimica Acta*, **71,** 3812–3832.

Kitchen, N. E. & Valley, J. W., 1995. Carbon isotope thermometry in marbles of the Adirondack Mountains New York. *Journal of Metamorphic Geology*, **13,** 577–594.

McLelland, J. M., Bickford, M. E., Hill, B. M., Clechenko, C. C., Valley, J. W. & Hamilton, M. A., 2004. Direct dating of Adirondack massif anorthosite by U-Pb SHRIMP analysis of igneous zircon: implications for AMCG complexes. *Geological Society of America Bulletin*, **116,** 1299–1317.

McLelland, J. M., Daly, J. S. & McLelland, J. M., 1996. The Grenville orogenic cycle (ca. 1350–1000 Ma): an Adirondack perspective. *Tectonophysics*, **265,** 1–28.

McLelland, J. M., Hamilton, M. A., Selleck, B. W., McLelland, J. M., Walker, D. & Orrell, S., 2001. Zircon U-Pb geochronology of the Ottawan Orogeny, Adirondack Highlands, New York: regional and tectonic implications. *Precambrian Research*, **109,** 39–72.

McLelland, J. M. & Husain, J., 1986. Nature and timing of anatexis in the eastern and southern Adirondack Highlands. *Journal of Geology*, **94,** 17–25.

McLelland, J. M. & Isachsen, Y. W., 1986. Synthesis of geology of the Adirondack Mountains, New York, and their tectonic setting within the southwestern Grenville Province. In: *The Grenville Province. Geological Association of Canada, Special Paper 31* (eds Moore, J., Davidson, A. & Baer, A.), pp. 75–94. Geological Association of Canada, St. John's, Newfoundland.

Mezger, K., Essene, E. J., van der Pluijm, B. A. & Halliday, A. N., 1993. U-Pb geochronology of the Grenville Orogen of Ontario and New York: constraints on ancient crustal tectonics. *Contributions to Mineralogy and Petrology*, **114,** 13–26.

Moore, J. M., Jr & Thompson, P. H., 1980. The Flinton Group: a late Precambrian metasedimentary succession in the Grenville Province of eastern Ontario. *Canadian Journal of Earth Sciences*, **17,** 1685–1707.

Morrison, J. & Valley, J. W., 1988. Post-granulite facies fluid infiltration in the Adirondack Mountains. *Geology*, **16,** 513–516.

Page, F. Z., Fu, B., Kita, N. T., Fournelle, J. H., Spicuzza, M. J., Schulze, D. J., Viljoen, F., Basei, M. A. S. & Valley, J. W., 2007a. Zircons from kimberlite: new insights from oxygen isotopes, trace elements, and Ti in zircon thermometry. *Geochimica et Cosmochimica Acta*, **71,** 3887–3903.

Page, F. Z., Ushikubo, T., Kita, N. T., Riciputi, L. R. & Valley, J. W., 2007b. High-precision oxygen isotope analysis of picogram samples reveals 2 μm gradients and slow diffusion in zircon. *American Mineralogist*, **92,** 1772–1775.

Pearce, N. J. G., Perkins, W. T., Westgate, J. A., Gorton, M. P., Jackson, S. E., Neal, C. R. & Chenery, S. P., 1997. A compilation of new and published major and trace element data for NIST SRM 610 and NIST SRM 612 glass reference materials. *Geostandards Newsletter*, **21,** 115–144.

Peck, W. H. & Valley, J. W., 2004. Quartz–garnet isotope thermometry in the southern Adirondack Highlands (Grenville Province, New York). *Journal of Metamorphic Geology*, **22,** 763–773.

Peck, W. H., Valley, J. W., Corriveau, L., Davidson, A., McLelland, J. M. & Farber, D. A., 2004. Oxygen-isotope constraints on terrane boundaries and origin of 1.18–1.13 Ga granitoids in the southern Grenville Province. In: *Proterozoic Tectonic Evolution of the Grenville Orogen in North America (Memoir 197)* (eds Tollo, R.P., Corriveau, L., McLelland, J.M. & Bartholomew, M.J.), pp. 163–182. Geological Society of America, Boulder, CO.

Rubatto, D., 2002. Zircon trace element geochemistry: partitioning with garnet and the link between U-Pb ages and metamorphism. *Chemical Geology*, **184,** 123–138.

Rubatto, D. & Hermann, J., 2007. Experimental zircon/melt and zircon/garnet trace element partitioning and implications for the geochronology of crustal rocks. *Chemical Geology*, **241,** 38–61 (doi:10.1016/j.chemgeo.2007.01.027).

Schaltegger, U., Fanning, C. M., Günther, D., Maurin, J.-C., Schulmann, K. & Gebauer, D., 1999. Growth, annealing and recrystallization of zircon and preservation of monazite in high-grade metamorphism: conventional and in-situ U-Pb isotope, cathodoluminescence and microchemical evidence. *Contributions to Mineralogy and Petrology*, **134,** 186–201.

Selleck, B. W., McLelland, J. M. & Bickford, M. E., 2005. Granite emplacement during tectonic exhumation: the Adirondack example. *Geology*, **33,** 781–784.

Spear, F. S., Kohn, M. J. & Cheney, J. T., 1999. *P-T* paths from anatectic pelites. *Contributions to Mineralogy and Petrology*, **134,** 17–32.

Spear, F. S. & Markussen, J. C., 1997. Mineral zoning, *P-T-X-M* phase relations and metamorphic evolution of some Adirondack granulites, New York. *Journal of Petrology*, **38,** 757–783.

Spicuzza, M. J., Valley, J. W., Kohn, M. J., Girard, J. P. & Fouillac, A. M., 1998a. The rapid-heating, defocused beam technique: a CO_2-laser-based method for highly precise and accurate determination of $\delta^{18}O$ values of quartz. *Chemical Geology*, **144,** 195–203.

Spicuzza, M. J., Valley, J. W. & McConnell, V. S., 1998b. Oxygen isotope analysis of whole rock via laser fluorination: an air-lock approach. *GSA Abstracts with Programs*, **30,** 80.

Storm, L. C. & Spear, F. S., 2005. Pressure, temperature and cooling rates of granulite facies migmatitic pelites from the southern Adirondack Highlands, New York. *Journal of Metamorphic Geology*, **23,** 107–130.

Tirone, M., Ganguly, J., Dohmen, R., Langenhorst, F., Hervig, R. L. & Becker, H.-W., 2005. Rare earth diffusion kinetics in garnet: experimental studies and applications. *Geochimica et Cosmochimica Acta*, **69,** 2385–2398.

Ushikubo, T., Kita, N. T., Cavosie, A. J., Wilde, S. A., Rudnick, R. L. & Valley, J. W., 2008. Lithium in Jack Hills zircons: evidence for extensive weathering of Earth's earliest crust. *Earth and Planetary Science Letters*, **272,** 666–676.

Valley, J. W., 2001. Stable isotope thermometry at high temperatures. In: *Stable Isotope Geochemistry* (eds Valley, J.W. & Cole, D.R.) *Reviews in Mineralogy and Geochemistry*, Vol. 43, pp. 365–414. Mineralogical Society of America, Washington, DC.

Valley, J. W., 2003. Oxygen isotopes in zircon. In: *Zircon* (eds Hanchar, J.M. & Hoskin, P.W.O.) *Reviews in Mineralogy and Geochemistry*, Vol. 53, pp. 343–386, Mineralogical Society of America, Washington, DC.

Valley, J. W., Bindeman, I. N. & Peck, W. H., 2003. Empirical calibration of oxygen isotope fractionation in zircon. *Geochimica et Cosmochimica Acta*, **67,** 3257–3266.

Valley, J. W., Bohlen, S. R., Essene, E. J. & Lamb, W., 1990. Metamorphism in the Adirondacks: II. The role of fluids. *Journal of Petrology*, **31,** 555–596.

Valley, J. W., Chiarenzelli, J. R. & McLelland, J. M., 1994. Oxygen isotope geochemistry of zircon. *Earth and Planetary Science Letters*, **126,** 187–206.

Valley, J. W., Kitchen, N. E., Kohn, M. J., Niendorf, C. R. & Spicuzza, M. J., 1995. UWG-2, a garnet standard for oxygen isotope ratios: strategies for high precision and accuracy with laser heating. *Geochimica et Cosmochimica Acta*, **59,** 5223–5231.

Valley, J. W., Lackey, J. S., Cavosie, A. J., Clechenko, C. C., Spicuzza, M. J., Basei, M. A. S., Bindeman, I. N., Ferreira, V. P., Sial, A. N. & King, E. M., 2005. 4.4 billion years of crustal maturation: oxygen isotope ratios of magmatic zircon. *Contributions to Mineralogy and Petrology*, **150,** 561–580.

Vielzeuf, D., Champenois, M., Valley, J. W., Brunet, F. & Devidal, J. L., 2005a. SIMS analyses of oxygen isotopes: matrix effects in Fe–Mg–Ca garnets. *Chemical Geology*, **223,** 208–226.

Vielzeuf, D., Veschambre, M. & Brunet, F., 2005b. Oxygen isotope heterogeneities and diffusion profile in composite metamorphic-magmatic garnets from the Pyrenees. *American Mineralogist*, **90,** 463–472.

Wasteneys, H., McLelland, J. M. & Lumbers, S., 1999. Precise zircon geochronology in the Adirondack Lowlands and implications for revising plate-tectonic models of the Central Metasedimentary Belt and Adirondack Mountains, Grenville Province, Ontario and New York. *Canadian Journal of Earth Sciences*, **36,** 967–984.

Wiedenbeck, M., Hanchar, J. M., Peck, W. H., *et al.*, 2004. Further characterisation of the 91500 zircon crystal. *Geostandards and Geoanalytical Research*, **28,** 9–39.

Wiener, R. W., McLelland, J. M., Isachsen, Y. W. & Hall, L. M., 1984. Stratigraphy and structural geology of the Adirondack Mountains, New York: review and synthesis. In: *The Grenville Event in the Appalachians and Related Topics, Special Paper 194* (ed. Bartholomew, M.J.), pp. 1–55. Geological Society of America, Boulder, CO.

Williams, I. S., 2001. Response of detrital zircon and monazite, and their U–Pb isotopic systems, to regional metamorphism and host-rock partial melting, Cooma Complex, southeastern Australia. *Australian Journal of Earth Sciences*, **48,** 557–580.

Wright, K., Freer, R. & Catlow, C. R. A., 1995. Oxygen diffusion in grossular and some geological implications. *American Mineralogist*, **80,** 1020–1025.

Received 24 April 2008; revision accepted 14 November 2008.

SUPPORTING INFORMATION

Additional Supporting Information may be found in the online version of this article:

File 1. Detailed sample site characterizations.

Figure S1. Linear correction plot for IMF correction.

Table S1. Details of garnet standards for IMF calculations.

Table S2. Raw data from major element electron microprobe traverses across garnet in thin section.

Table S3. Normalized garnet compositions from garnet in thin section, calculated as 12 oxygen.

Table S4. XRF analyses of leucocratic material.

Table S5. Molecular norms calculated from XRF data (McBirney, 1993).

Table S6. Laser fluorination $\delta^{18}O$ analyses of bulk quartz and garnet separates and apparent $\Delta^{18}O$ temperatures.

Table S7. $\delta^{18}O$ analyses by ion microprobe of dated zircon, as well as growth zone and pit characterizations.

Table S8. $\delta^{18}O$ analyses by ion microprobe of garnet in thin sections, pit observations and major element compositions used to calculate IMF corrections.

Table S9. Chondrite-normalized REE and raw trace element concentrations in dated zircon.

Table S10. Chondrite-normalized REE and raw trace element concentrations in zircon co-existing with garnet in thin section.

Table S11. Chondrite-normalized REE and raw trace element concentrations in garnet co-existing with zircon in thin section.

Table S12. Summary of *t*-tests applied to average zircon $\delta^{18}O$ values from corresponding leucosome-melanosome pairs.

Please note: Wiley-Blackwell are not responsible for the content or functionality of any supporting materials supplied by the authors. Any queries (other than missing material) should be directed to the corresponding author for the article.